What Causes Tides ?

Yongfeng Yang
Bureau of Water Resources of Shandong Province, Jinan, 250014, CHINA

Abstract. It has been known for thousands of years that the waters of coastal seas ebb and flow on a daily basis. This movement was long-term ascribed to the gravitational pulls of the moon and sun on the water. However, an in-depth investigation shows this understanding to be incomplete. Here we propose, the earth's curved motions about the centre of mass of the earth-moon system and around the sun create some centrifugal effects to stretch its body, under the effect of the deformation, the rotating earth drives its each part to regularly move up and down, giving birth to oscillations for ocean basins, generating water transferring and further the rise and fall of regional water levels.

1. Introduction

a. A brief retrospect of tidal theories

From antiquity it has been known that coastal seas always perform daily regular water movements of rise and fall. Since these movements are closely related to the frequently coastal activities, explaining them has undoubtedly tested human wisdom. Aristotle (384-322 BC) was highly perplexed by the phenomenon and vaguely attributed it to the rocky nature of the coastline. The early Chinese considered tides as the beating of the earth's pulse and alternately, it was believed to be caused by the earth's breathing. Others thought tides were caused by the different depths of ocean water. Galileo theorized that the rotations of the earth around the sun and about its axis induced motion within the sea to generate the tides. The majority certainly linked tidal action to the influence of the moon and of the sun. Seleucus (2nd century BC) was the first to consider this connection. He concluded the height of tide was correlated with the moon's position relative to the sun. However, the exact determination of how the moon and sun caused tides was unknown. A few Arabic explanations proposed that the moon used its rays to heat and expand the water. Descartes argued that space was full of ethereal substance and the resulting stresses between the ether and the earth's surface gave birth to tides when the moon orbited the earth. In contrast, Kepler and Newton defined the action as the attraction of the moon and sun on the water. Newton concluded the moon's gravitation caused a pair of water bulges on the earth. In consideration of the complexity of actual oceans and currents, Laplace developed a set of hydrodynamic equations. Together with the following endeavours (made by William Thomson, Baron Kelvin, Henri Poincaré, Arthur Thomas Doodson, etc.,), the idea of the gravitational attractions of the moon and sun on the water (the attractive mechanism) was increasingly consolidated and became the cornerstone of modern tidal theories. A fuller review of tidal theory may be seen in these works (Pugh 1987; Cartwright 1999; Deacon 1971; Pugh and Woodworth 2014). Undoubtedly, the physics of tides involve a variety of fields ranging from the orbit of celestial objects (the moon

and the sun, for instance), the mixing of the oceans, solid-earth geophysics and coastal flooding (Lambeck 1988; Munk 1997; Vlasenko et al. 2005). In the past decades a rapid growth of tide mode greatly facilitated spatial and ground measurements (Pekeris et al. 1969; Schwiderski 1979; Fu and Cazenave 2001; Visser et al. 2010), tidal dynamics and energy dissipation were also studied (Stammer et al. 2014), the investigation on internal tides becomes considerably active (Gargett and Hghes 1972; Phillips 1974; Shepard 1975; Garrett and Munk 1979; Gao et al. 2013; Shanmugam 2014), these, in turn, help realize a better understanding of tide. Even so, many problems still remain open in the established tidal theories.

b. Problems of the established tidal theories

The established tidal theories may be morphologically divided into two parts: the equilibrium tide and the dynamic tide. The equilibrium tide theory was directly developed from Newton's law of gravity: the earth orbits about the centre of mass of the earth-moon system, this makes all particles of the earth travel around in circles which have the same radius. The force responsible for these circular or curved motions is treated as centripetal force. The centripetal force necessary to maintain each particle of the earth in this revolution is the same as for the particles at the centre. For particles nearer the moon, its gravitational attraction on them is greater than the centripetal force. Further away, the moon's gravitational attraction is weaker than the centripetal force. The difference between the centripetal force and the moon's gravitational attraction is the tide-generating force (Pugh 1987; Pugh and Woodworth 2014). The tide-generating force is further decomposed into two components respectively: perpendicular and parallel to the earth's surface. The vertical component can be compensated by earth's gravity, but the horizontal component cannot be counteracted in the same manner and therefore causes particles to move in the direction of the force. The net result of the tidal forces acting on a watery earth is to move water towards positions nearest to and farthest from the moon. This eventually generates two bulges of elevated water along the earth-moon line and a depression of the water in a ring around the earth halfway between the bulges (Pugh 1987; Robert 2008; Pugh and Woodworth 2014). For an earthly site it would pass through the two bulges and the depression as the Earth spins, and hence undergo two cycles of high and low water per day. The equilibrium tide yields several points that don't agree with observation.

First of all, the two bulges yield an equality of two successive low water levels and an inequality of two successive high water levels for a site. As shown in Fig. 1 (a), there is a ring (marked with white) of lowest water level that is mechanically formed midway between the two bulges, a site P which would pass through this ring at P_1 and P_2 and through the two bulges at P and P'. As the earth spins, two low water levels of the same size and two high water levels of different size are generated for this site per day. From the viewpoint of the globe, other sites such as N and Q, which are at different latitudes, also would pass through this ring respectively at $N_1(N_2)$ and $Q_1(Q_2)$ to undergo two low water levels of same size. On the whole, the structure of the two bulges requires the high water levels of all sites to be different in size and the low water levels to be the same size within a fixed day. Contrary to this, the low waters of the observed tides are generally different in size.

Secondly, the two bulges require the sizes of two successive high water levels to be developed in reverse during a lunar month, namely, for a site which is at a higher latitude, the size of one high water level is increased/decreased whereas the size of another is decreased/increased when the two bulges transfer between north and south. This behaviour may be easily seen from Fig. 1 (a). Refer to Pugh's work (1987), the tide-generating force was eventually developed into a formula below to describe the elevation of the sea surface.

$$H_m=a(M_m/M_e)[C_0(t)(3\sin^2\varphi_p/2-1/2)+C_1(t)\sin 2\varphi_p+C_2(t)\cos^2\varphi_p]$$

$$C_0(t)=(a/R_m)^3(3\sin^2 d/2-1/2)$$

$$C_1(t)=(a/R_m)^3(3\sin 2d\cos C_p/4)$$

$$C_2(t)=(a/R_m)^3(3\cos^2 d\cos 2C_p/4)$$

where H_m, a, M_m, M_e, φ_p, R_m, d, and C_p are respectively the elevation of the sea surface, the earth's radius, the moon's mass, the earth's mass, the latitude of a particle at the sea's surface, the distance of the earth and moon, the declination of the moon, and the hour angle of the particle relative to the moon.

By replacing M_m and R_m respectively with M_s (the sun's mass) and R_s (the distance of the earth and sun), the elevation of the sea surface H_s due to the effect of the sun may be gotten. $H_m+ H_s$ therefore represent the total elevation of the sea surface due to the influences of the moon and sun. Fig. 1(b) exhibits several tides expected from the tide-generating forces. Related parameters for this expectation are listed in Table 1. It can be seen that, at latitude 30°N the size of one high water level of the expected tide increases or decreases when the size of another high water decreases or increases during the month; towards higher latitudes (60°N and 80°N, for instance) this asymmetry is developed considerably. Contrary to these, the tide records in Fig. 1(c) show that the two successive high water levels of each of the observed tides are alternately increased or decreased. This symmetry is also applicable for the two successive low water levels. Morphologically speaking, there is a significant discrepancy between the expected tides and the observed tides.

Thirdly, refer to Fig. 1(a), the two bulges require semidiurnal tides (which have two high waters and two low waters of same size per day) to occur at lower latitudes, diurnal tides (which have one high water and one low water of same size per day) to occur at higher latitudes, and mixed tides (which have two high waters and two low waters of different size per day) to occur at middle latitudes. Contrary to this, the tide distributions in Fig. 1(e) show that the semidiurnal and mixed tides are almost dominant around the globe. Only a few places (the Karumba and Mexico gulf, for instance) hold diurnal tides.

Fourthly, there is a big tidal range difference between ocean tides and continental shelf tides. The tidal range expected from the tide-generating forces is about 0.5 m at the equator. Contrary to this, in the main oceans the observed tides have an average range of about 0.0~1.0 m, while in the continental shelf seas a much larger range of tides are observed. At some places (the Bay of Fundy and the Argentine shelf, for instance) the tidal ranges may even reach 10.0 m (Pugh 1987; Pugh and Woodworth 2014).

Lastly, the tide-generating forces require the larger tide to occur at lower latitude and the smaller tide to occur at higher latitude. Refer to Fig.1(b), the ranges of the tides

generated from the tide-driving forces trend to become smaller and smaller as latitude increases. Contrary to this, the ranges of the observed tides are generally uniform.

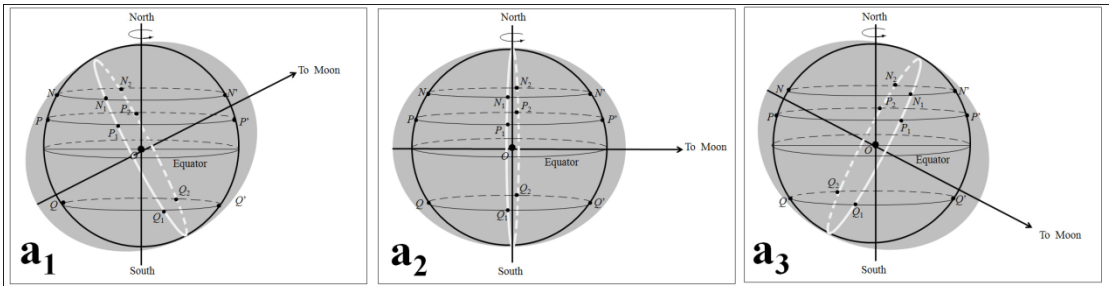

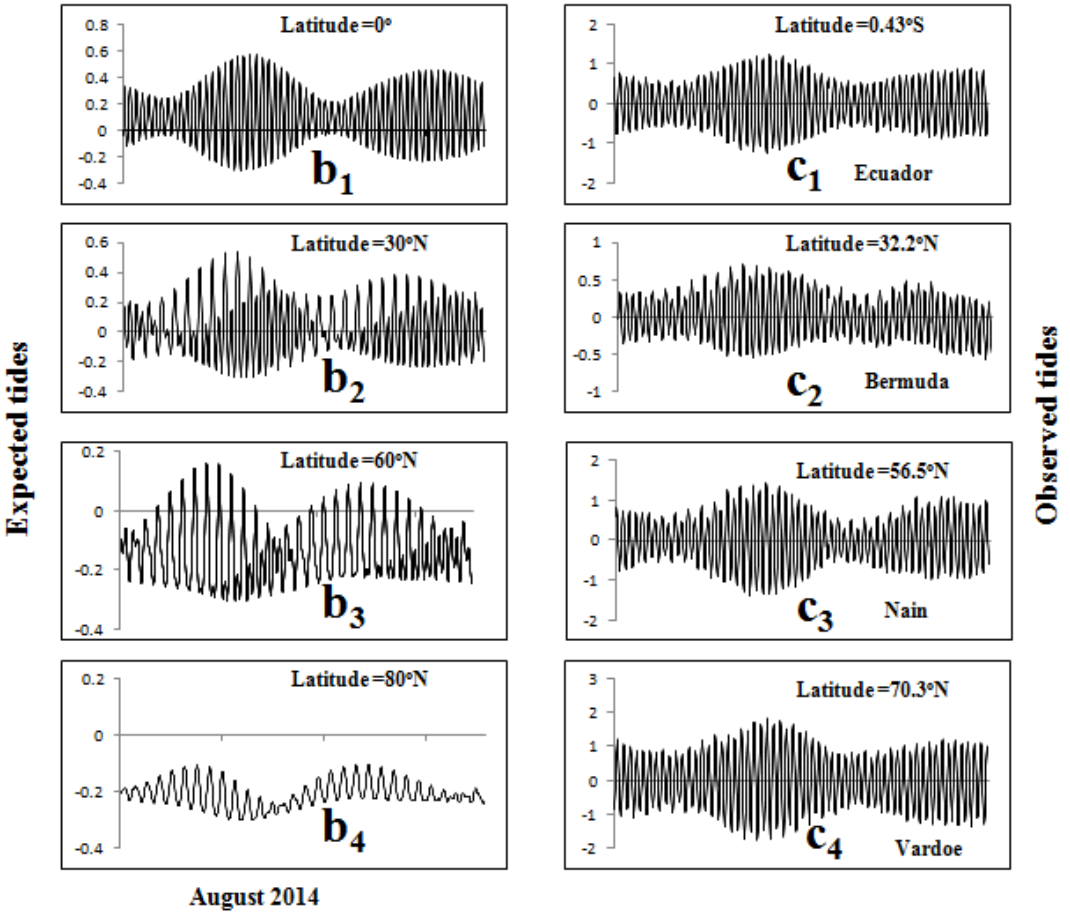

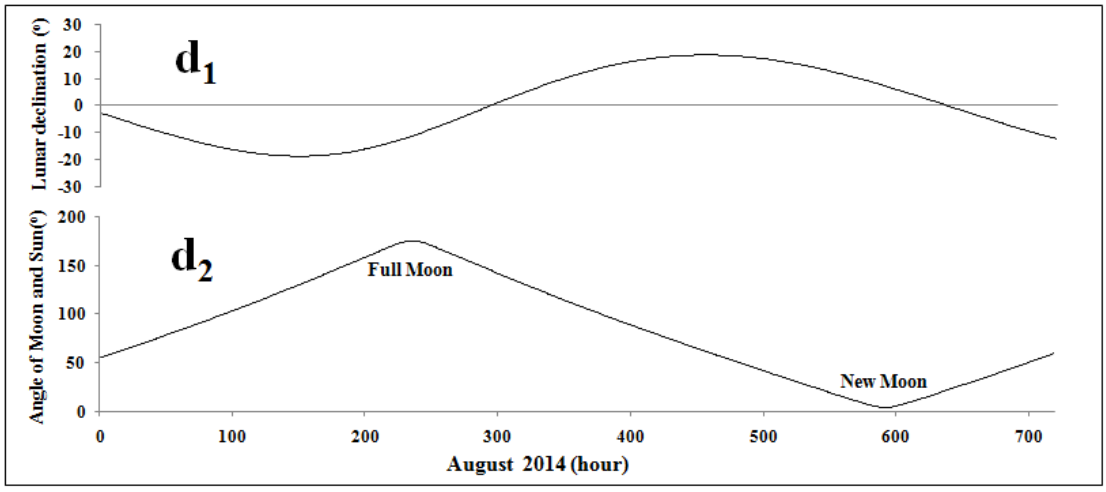

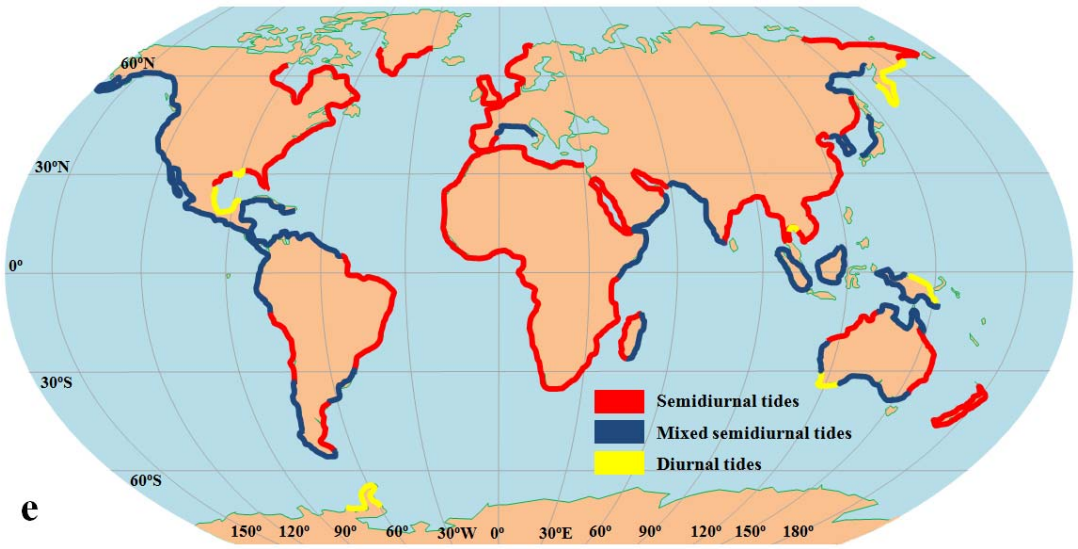

FIG. 1. Comparison of the expected tides from the attractive mechanism and observations. a, showing how the unequal high water levels and the equal low water levels are generated at various sites under the resulting two bulges. From $\mathbf{a}_1$, $\mathbf{a}_2$, to $\mathbf{a}_3$, it represents the orderly positions of the two bulges as the moon transfers from the north to the south. *O* is the earth's centre. The big circle represents an undisturbed watery planet. Note that the two bugles are seriously exaggerated; **b**, the expected tides from the tide-generating forces at different latitudes in August 2014.Vertical axis represents tidal amplitude and unit is metre; **c**, the observed tides at different latitudes during the month. Vertical axis represents tidal amplitude and unit is metre; **d**, the positions of the moon and sun relative to the earth in the month; **e**, tidal pattern distribution of the observed tides throughout the globe. Data supporting is from U.S. NOAA, GLOSS database - University of Hawaii Sea Level Center, and Bureau National Operations Centre (BNOC) of Australia.

Several factors haven't been considered in the equilibrium tide. If there is no landmass, the tidal bulges would continuously track from east to west with the earth's diurnal rotation. The presence of landmasses completely breaks off this progression. Most of the continents are oriented in the north-south direction, the travelling tidal wave would encounter continents, generating a reflection of tidal wave. From deep oceans to shelf seas, water becomes shallow, the slope of the sea floor also greatly disperses and refracts tidal waves. In addition, the Coriolis force deflects tidal waves to right in the direction of motion in the northern hemisphere and to left in the direction of motion in the southern hemisphere. Within the constraint of these influences, the dynamic tide was developed. An earlier treatment of this matter was made by Laplace who expanded the equilibrium tide into a set of hydrodynamic equations of continuity and momentum. He assumed a spherical earth with a geocentric gravitational field, a rigid ocean bottom and a shallow ocean which allowed Coriolis accelerations to be neglected (Pugh 1987; Pugh and Woodworth 2014). These hydrodynamic equations are followed by a series of ideas such as progressive and standing wave, resonance, Kelvin wave, and amphidromic system. Wave has crest (high) and trough (low), this feature resembles the characteristic of tide (high and low water), treating tide as wave is theoretically acceptable. Wave may propagate, reflect, and refract. If the frequencies of two waves

are close to each other, a resonance between them may amplify amplitude. A long progressive wave can be constrained by the combination of the Coriolis force and the shore to form a Kelvin wave that often moves cyclonically around a basin. Especially, at the boundary of a basin two Kelvin waves travelling in opposite directions may been seen forming an amphidromic system. Based on these theoretical ideas, a general understanding is achieved: ocean tides are generated directly by the external gravitational forces, the continental shelf tides were generated by co-oscillation with oceanic tides (Pugh 1987; Pugh and Woodworth 2014).

Careful readers would find, the equilibrium tide tells why there would be the variation of high and low water on the earth whereas the dynamic tide tells how the high and low water moves around the earth. Essentially, the dynamic tide hasn't resolved the problems of the equilibrium tide we demonstrated above, except for the introduction of a resonance mechanism which attempts to deal with the problem of tidal range difference between ocean tides and continental shelf tides. However, it is still not successful. Supposedly, the oceanic tidal waves have spread onto the continental shelf seas, but their resonances with local oscillations are not easy to happen as thought, this is because the resonance of two waves has a strictly physical constraint. An approach of frequency (also wavelength) is simply not enough. At least, the phase of two waves must be the same. For example, if the wavelengths of two sinusoidal waves are the same but the phase between them has a difference of 180^o, the amplitude of the combined wave would be zero, this is a minification but not an amplification. This point may be demonstrated with the composition of two sinusoidal waves $\sin(2\omega t)$ (the natural) and $\sin(2\omega t+k45)$ (the forced), which resemble the semidiurnal tides, the natural and the forced conceptually represent the oscillation of the continental shelf sea and the oceanic tidal wave, respectively, where ω is angular speed of unit degree per hour, and $\omega = 15^o$, t is the time of unit hour, $k45$ is phase lag of unit degree, k=0, 1, 2, 3, 4, 5, 6, 7, and 8. It can be seen in Fig. 2 that the amplitudes of some of the combined waves are greatly suppressed when phase lag is between 135^o~225^o, in particular, the amplitude reduces to zero when phase lag is 180^o. The amplitudes can be amplified when the phase lag is between 0^o~135^o and between 225^o~360^o.

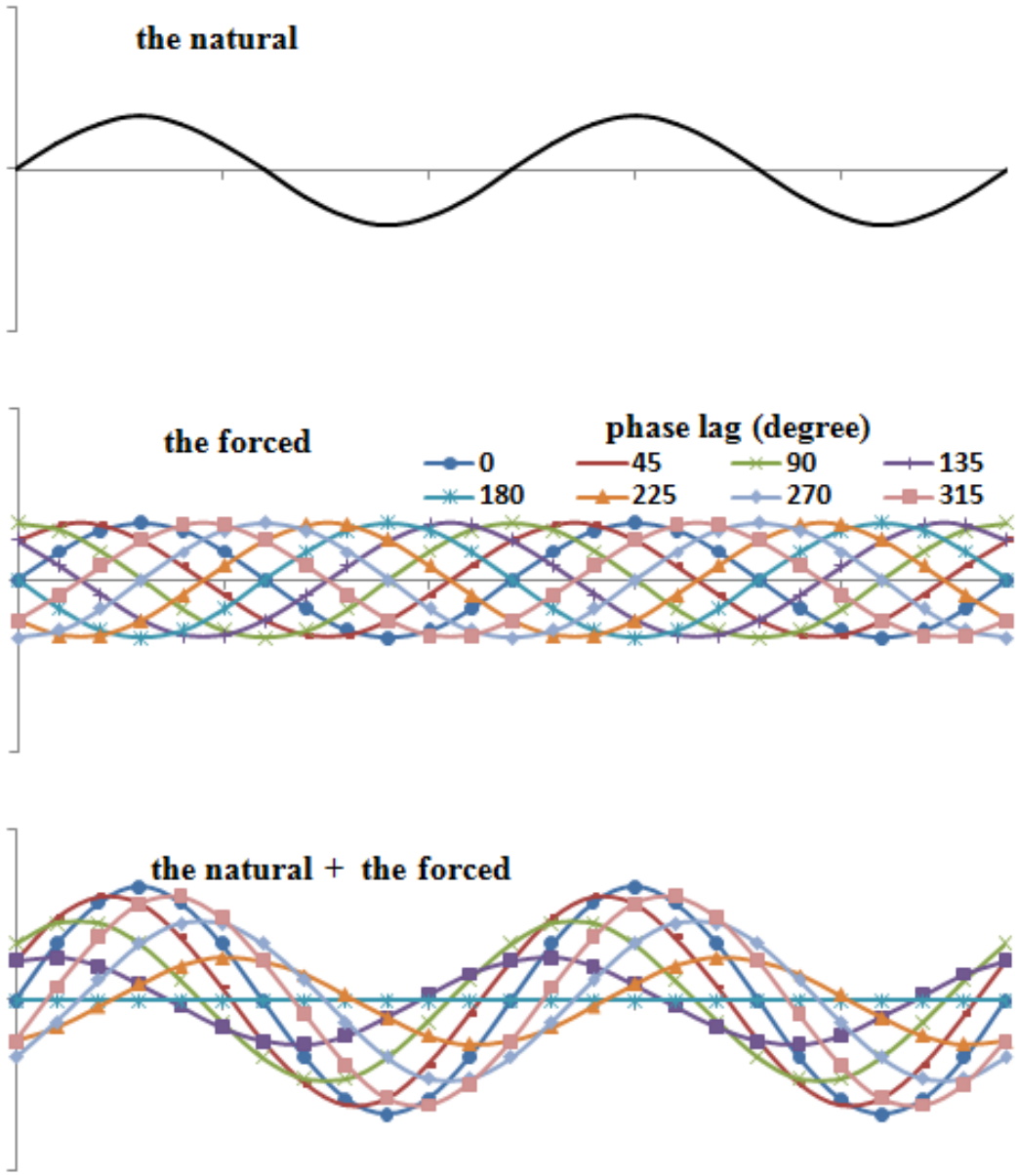

FIG. 2. Modelling the resonance of natural oscillation and forced oscillation under different phase lag.

The demonstration above leads to the fact that a system, which is forced by oscillation close to its natural period, is uncertain to yield a large amplitude anywhere. One should be aware that, due to the moon's advance in its orbit, the gravitational pull of the moon on an earthly site has a phase (time) lag of about 52 minutes per day (equivalent to 3.75^{o}). This means that, after 36 days the total phase lag falls into a span of 135^{o}~225^{o}, in which a counteraction of the forced and the natural will be made. In other words, to realize the resonance of the oceanic tidal wave and the natural oscillation of the continental shelf sea, the latter has to timely recede so as to keep synchronization with the former. This hence leads to a problem why the natural oscillation of the continental shelf sea may recede day by day. It is unintelligible because the natural (inherent)

oscillation of a system doesn't advance or recede. One must also be aware that, in the real world the occurrences of resonated events (collapsing bridge, acoustic speaker, for instance) are rare, there are no eternal resonances for a special system. Attempting to relate resonance to tide appears to greatly violate our intuition.

For a long time, too much attention was paid to ocean tide whereas the deformation of solid Earth (also called Earth tide) was less considered. This situation changed since last century. Love (1909) presented the first theory of earth tide when he was accounting for nutations. Longman (1963) introduced a Green's function by which the surface deformation of the earth can be calculated exactly. Subsequently, these authors (Hendershott 1972; Farrell 1973; Melchior 1974; Agnew 1981; Scherneck 1991) systematically investigated the responses of earth tide to the tide-generating forces and to ocean tide. The surface of solid earth holds ocean, any deformation of solid earth would inevitably disturb ocean. It's believed that, under the effect of the gravitational pulls of the moon and sun, the elastic earth follows the shape of the equilibrium tide, its influence on ocean tide may be expressed with $(1+k-h)\Omega p/g$, where $\Omega p/g$ is the equilibrium tide amplitude, $(1+k-h)$ is a diminishing factor (combination of Love numbers) in the equilibrium tide (Pugh 1987; Pugh and Woodworth 2014). This treatment, however, lost a significant point. As $(1+k-h)\Omega p/g$ itself represents a variation of tidal amplitude, this means the contribution of the deformation of solid earth to ocean tide is a simple reduction of tidal amplitude in the vertical direction. Actually, solid earth responds quickly to the external forces. Once solid earth deforms, it would drive each part of ocean basin to move up/down, under the effect of the earth's gravity, water begins to mechanically flow. For a site of ocean basin, the inflow of water increases water level whereas the outflow of water decreases water level, tide therefore happens. In the following sections we investigate this movement and further explain tide.

2. An analytic treatment of the deformation of solid earth

The earth may be mechanically thought to be a solid sphere that is enveloped by water and atmosphere (Fowler 2004; National Research Council 1964, 1993). The structure of solid earth, from surface to interior, is sequentially divided into crust, mantle, outer core, and inner core (Jordan 1979). A large number of works confirmed that these layers are filled with various materials (Wootton 2006; Stixrude and Cohen 1995; Ozawa et al. 2011; Herndon 1980; Herndon 2005; Birch 1964) and denser materials are gravitationally concentrated towards the interior (Monnereau et al. 2010). Notwithstanding, solid earth is strictly not a rigid body. Both experiments and measurements have proved it to be elastic (Stixrude and Cohen 1995; Schettino 2014) and to have been stretched into an oblate spheroid because of the centrifugal effect of the earth's rotation about its axis (Heiskanen 1962; Burša 1993). It is well known that the earth orbits about the centre of mass of the earth-moon system and the earth-moon system orbits about the sun. Fuller details of the motions of the earth, moon, and sun may be seen in other works (Kopal 1969; Schureman 1976; Smart 1940; Doodson and Warburg 1941; Kaula 1968; Roy 1978). These two curved motions mechanically generate two centrifugal effects F_1 and F_2 for solid earth (Fig. 3(a_1)). F_1 and F_2 are

respectively balanced by the gravitational attraction from the moon f_1 and from the sun f_2. If we define the centrifugal effect of the earth's rotation about its axis as F_3, then the ratio between F_1, F_2, and F_3 will be 1:178:505 according to established parameters, such as orbital radius, orbital period, mass of each body, and so on. Practically, F_2 is far greater than F_1, but the difference is that F_2 is not at the earth's centre where F_1 is fixed. In consideration of this matter, we suppose the effective part of F_2, which is able to stretch the earth, is relatively small and lies at the earth centre (O_1). The counteraction of F_1 (F_2) and f_1 (f_2) finally results in the fact that solid earth is physically elongated in the earth-moon (sun) line (Fig. 3(a_2 and a_3)). We call it lunar (solar) deformation in the following sections. Under such a deformation, an earthly site will undergo a change of rise and fall as the earth spins on its axis.

We assume solid earth to be a standard sphere and use the centrifugal effects F_1 and F_2 to independently stretch it along the earth-moon line (O_1M) and the earth-sun line (O_1S). Under the centrifugal effect F_1, section GIHJ which passes through earthly site M, becomes section G'I'H'J', section KQLP becomes section K'Q'L'P', site M turns to site M'. Section GIHJ is geometrically perpendicular to section KQLP, GH is the intersecting line between them (Fig. 3(b_1, b_2, and b_3)); Under the centrifugal effect F_2, section VSWR which also passes through site M and section TYUX respectively become sections V'S'W'R' and T'Y'U'X', site M turns to site M'', section VSWR is perpendicular to section TYUX, VW is the intersecting line between them (Fig. 3(c_1, c_2, and c_3)). It can be seen that solid earth simultaneously undergoes two elongations (respectively in the direction of the earth-moon line and in the direction of the earth-sun line) and two compressions (respectively in the direction of section KQLP and in the direction of section TYUX). Hence, the final position of site M (relative to the earth's centre) is a result of the combination of these adjustments (elongations and compressions). According to the geometry of the ellipse, the distance of site M and the earth's centre may be expressed as

$$H = O_1\mathrm{M}' + O_1\mathrm{M}'' - O_1\mathrm{M} \quad (1)$$

$$O_1\mathrm{M}' = [\mathrm{I}'O_1^2\cos^2\beta + \mathrm{G}'O_1^2\sin^2\beta]^{1/2} \quad (2)$$

$$O_1\mathrm{M}'' = [\mathrm{S}'O_1^2\cos^2\gamma + \mathrm{V}'O_1^2\sin^2\gamma]^{1/2} \quad (3)$$

Where

I'O_1 and G'O_1 are the semi-major and semi-minor axis of ellipse G'I'H'J', respectively, and GO_1= IO_1, G'O_1= GO_1-k_m', I'O_1= IO_1+k_m, k_m is the elongation of solid earth in the direction of the earth-moon line (O_1M) that is due to the centrifugal effect F_1, k_m' is the compression of solid earth in the direction of section KQLP, GO_1 (IO_1) is the mean radius of solid earth, equal to O_1M. β is the angle of site M and the moon relative to the earth's centre.

S'O_1 and V'O_1 are the semi-major and semi-minor axis of ellipse V'S'W'R', respectively, and VO_1= SO_1, V'O_1= VO_1-k_s', S'O_1= SO_1+k_s, k_s is the elongation of solid earth in the direction of the earth-sun line (O_1M) that is due to the centrifugal effect F_2, k_s' is the compression of solid earth in the direction of section TYUX, VO_1 (SO_1) is the mean radius of solid earth, equal to O_1M. γ is the angle of site M and the sun relative to the earth's centre.

β and γ are calculated through some astronomical constants. $\cos\beta = \sin\sigma\sin\delta_m + \cos\sigma\cos\delta_m\cos C_{mm}$, $\cos\gamma = \sin\sigma\sin\delta_s + \cos\sigma\cos\delta_s\cos C_{ms}$, where σ, δ_m, δ_s, C_{mm}, and C_{ms} are respectively the geographic latitude of site M, the declination of the moon, the declination of the sun, the hour angle of site M with respect to the moon, and the hour angle of site M with respect to the sun. The declination and right ascension of the moon and the sun may be gotten from the ephemeris or be calculated. The hour angle may be worked out through the positions of these bodies.

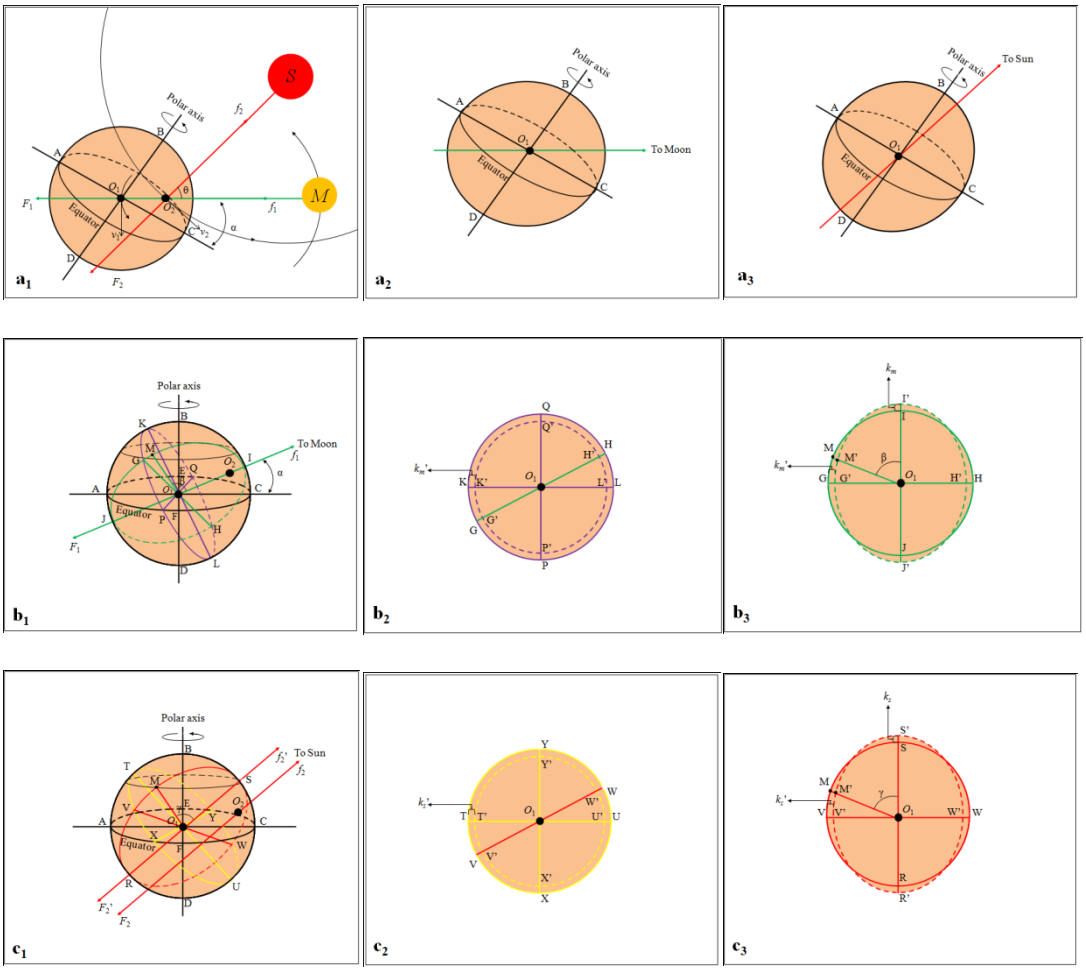

Figure 3. Combined centrifugal effects for solid Earth and the resulting deformation. a$_1$, the curved motions of the Earth around the barycenter of the Earth-Moon system and around the Sun, **a$_2$** and **a$_3$** are the resulting deformations respectively in the direction of the Earth-Moon line and in the direction of the Earth-Sun. F_1 and F_2 are the centrifugal effects solid Earth undergoes due to these curved motions. O_1, O_2, M, and S are the Earth's centre, the barycenter of the Earth-Moon system, the Moon, and the Sun, respectively. Θ is the angle between the Moon and the Sun relative to the barycenter of the Earth-Moon system. Section AECF is the equatorial plane, α is the Moon's declination. v_1 and v_2 are respectively the velocity of the Earth orbiting the barycenter of the Earth-Moon system and the velocity of the Earth-Moon system orbiting the Sun, which generate the centrifugal effects F_1 and F_2 that are anywhere balanced the gravitational attraction from the Moon f_1 and from the Sun f_2; **b$_1$, b$_2$,** and **b$_3$**, solid Earth under the effect of F_1 and the resulting deformations respectively in the direction of section KQLP and in the direction of the Earth-Moon line. Purple (green) real and dashed circles represent the original and disturbed shapes of solid Earth in the related directions; **c$_1$, c$_2$,** and **c$_3$**, solid Earth under the effect of F_2

(also F_2') and the resulting deformations respectively in the direction of section TYUX and in the direction of the Earth-Sun line. Line $F_2'f_2'$ is parallel to line F_2f_2, meaning the centrifugal effect F_2 and gravitational attraction f_2 are working on the Earth's centre (O_1). Yellow (red) real and dashed circles represent the original and disturbed shapes of solid Earth in the related directions.

The ratio of centrifugal effect F_3/F_1 is about 505:1. A rough evaluation based on this amount shows the centrifugal effect F_1 may generate an elongation of about 42.00 m for solid earth if the earth's oblate spheroid is referred. However, the earth's oblate spheroid is likely to be the result of an accumulative effect during a time scale of billions of years, thus, the centrifugal effect F_1 at an instant could give rise to only a slight amount. Here we assume the elongation of solid earth in the earth-moon line (due to the centrifugal effect F_1) at an instant to be 0.50 m at the time when the moon is at perigee and in the earth-sun line (due to the centrifugal effect F_2) at an instant to be 0.30 m, and assumes the compression to the elongation to be a factor of 1.0. The moon's elliptical orbit means a changing distance between the earth and the moon. As the centrifugal effect F_1 is at any point balanced by the moon's gravitation and the moon's gravitation is reversely proportional to the square of distance, the elongation of solid earth in the earth-moon line may thus be approximately expressed as $k_m=0.5R_m^2/R_{peri}^2$. For the elongation of solid earth in the earth-sun line it may be constant as the earth's orbit is nearly circular. And then, k_s=0.30 m, $k_m'=k_m$, $k_s'=k_s$, where k_m and k_s are respectively the elongation of solid earth in the earth-moon line and in the earth-sun line, k_m'and k_m' are respectively the compressions to the response of the elongations. Please note that practically, the elongation k_m (k_s) and compression k_m'(k_s') should be obtained by means of measurement.

The final deformation of solid earth is therefore a result of the combination of lunar and solar deformations, and may periodically vary due to the changes of the positions of the moon, sun, and earth. In particular, it becomes maximum at the times of full and new moon and minimum at the times of first quarter and last quarter. This is because at the times of full and new moon the two deformations add to each other to reinforce, whereas at the times of first quarter and last quarter the two cancel each other to weaken.

3.The water movement of an oscillating vessel

As shown in Fig. 4, we first let the right end of a rectangular water box rise, the water then flows towards left. If line MN represents a reference level, the water level at site M rises whereas the water level at site N falls. We further restore the right end to its former level and continue to let the left end rise, the water at the left end flows towards right, the water level at site M correspondingly falls whereas the water level at site N rises. Repeat the rise and fall of the two ends continuously, the water level of sites M and N alternately vary. Compared to sites M and N, another site S, which is in the middle of the vessel, holds the minimal variation of water level. Now we let one end rise and fall continuously while the other end is motionless, the water level at sites M and N still alternately vary. Further, we let one end rise (fall) and another end fall (rise) at the same time, the water level at sites M and N also alternately vary. The variation of

water level at one end may be approximately represented by the difference of vertical displacement between the two ends. Mathematically, this movement of high and low water in an oscillating vessel may be depicted with a sinusoidal wave.

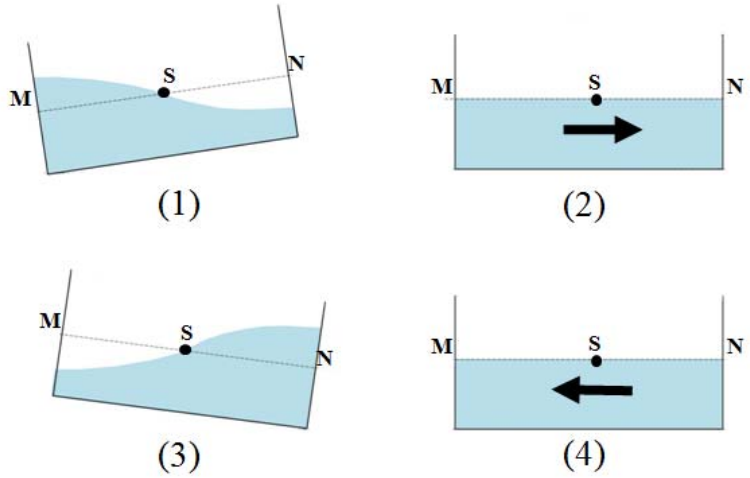

FIG. 4. Modelling the water movement of an oscillating rectangular box. From (1), (2), (3) to (4) it represents a full alternation of the rise and fall of the two ends. Arrows denote the directions of water movements.

4.The resulting tide

In the real world, about 71% of the earth's surface is covered with ocean (Pidwirny 2006). In appearance, all the oceans bisect the earth's surface, and each ocean basin is like a gigantic vessel of water. According to the arguments presented above, every part of ocean basin would rise and fall regularly as the deformed solid earth spins, this leads water to transfer back and forth, and also generates high and low water at the ends of ocean basin. The water transferring is conceptually depicted in Fig. 5. Within the lunar deformation of solid earth, there is an elongation in the direction of the earth-moon line and a compression in the midpoint of the elongation. The elongation of solid earth may be represented by two bulges. The first bulge would track from east to west along line *L* as the earth spins. For a coastal site W, the raising of site *a* firstly leads water to transfer towards site W. Subsequently, the raising of the site *b*, *c*, and *d*, which are assumed to be located at ocean floor, leads water to transfer from these sites to site W. With the passage of time, site *a*, *b*, *c*, and *d* begin to fall in order. This leads water to return, inevitably there is a water transferring from site W to each of these sites. Half a day later, the second bulge would track from east to west along line *L*', the raising of site *e*, *f*, *g*, and *h* (site *f* and *g* are also assumed to be located at the bottom of the ocean), leads water to flow out from these sites, transferring towards site W. Similarly, with the passage of time, these sites begin to fall in order, and cause water to transfer from site W to each of these sites. Please note in the day, each of sites *b*, *c*, *d, f*, and *g* would undergo a maximum rise and a maximum fall. Even if site *a*, *e*, and *h* can't undergo a maximum rising, the landmass's rise still would lead water to transfer towards site W, this may be ascribed to a spherical structure of the earth. Once the water transfers

between site W and each of these sites, this movement may be then treated as wave. The total variation of water level at site W may be expressed with a simple addition of these waves. This eventually provides foundation for the following expectations.

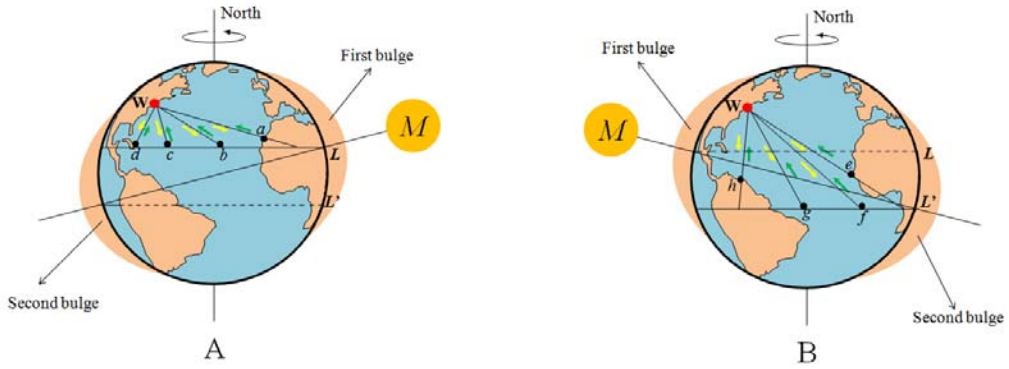

FIG. 5. A simplified system illustrates water transferring due to the rise and fall of related sites. From A to B, earth rotates 180^o with respect to the moon. Green (yellow) arrows denote the direction of water transferring between site W and the other sites. *L* and *L*' represent the path the earth-moon line tracks along the earth's surface (dashed line means at far side). The two bulges denote the elongation of solid earth.

Four sites (Karumba, Fort Point, Prince Rupert, Rorvik) are selected to display the variation of water levels. In consideration of the physics of the oscillating rectangular vessel and of the water transferring in the ocean, each of these sites acts as one end of a smaller rectangular vessel. One or more partners are employed as the other ends of these smaller vessels. The treatments of these vessels are outlined in Fig. 6(a). V_{11}, V_{21}, V_{31}, and V_{41} represent the four sites, V_{12}, V_{22}(V_{22}'), V_{32}, V_{33}, V_{34}, V_{35}, V_{36}, and V_{42} are their first partners. V_{13} is added as second partner of V_{11} because the rising or falling of V_{13} (which is at the northwest Celebes Sea) would lead water to transfer between V_{13} and V_{12}, from V_{12} the transferring can further move towards V_{11} or V_{13}. V_{32}, V_{33}, V_{34}, V_{35}, and V_{36} are added as first partners of V_{31} because the rise or fall of these sites, all would lead water to transfer between V_{31} and them. V_{43}, V_{44}, V_{45}, and V_{46} are added as second partners of V_{41} because the rise or fall of these sites would result in water transferring between V_{42} and them, from V_{42} the water transferring can further move towards V_{41} or these sites. As we demonstrated above, the maximum rising of solid earth is always in the direction of the earth-moon line and the paths the earth-moon line tracks the earth are along *L* and *L*', this means that the positions of V_{22}, V_{32}, V_{33}, V_{34}, V_{35}, V_{36}, V_{43}, V_{44}, V_{45}, and V_{46} are time-variable, relevant to the position of the moon. Some possible positions for them are marked with V_{22}', V_{32}', V_{33}', V_{34}', V_{35}', V_{36}', V_{43}', V_{44}', V_{45}', and V_{46}'. Through Google earth software, we got the geographic latitudes and longitudes of V_{11}, V_{12}, V_{13}, V_{21}, V_{31}, V_{41}, and V_{42}. The determination of the geographic latitudes and longitudes of V_{22} (V_{22}'), V_{32} (V_{32}'), V_{33} (V_{33}'), V_{34} (V_{34}'), V_{35} (V_{35}'), V_{36} (V_{36}'), V_{43} (V_{43}'), V_{44} (V_{44}'), V_{45} (V_{45}'), and V_{46} (V_{46}') is relatively complicated. Taking into account the paths that the earth-moon line tracks on the earth's surface, the latitude of V_{22} (V_{22}') is treated the same as the positive of the

moon's declination if the angle between V_{21} and the moon, relative to the earth's centre is less than 90^o and the same as the negative of the moon's declination if the angle is greater than 90^o, the longitude of V_{22} (V_{22}') is treated the same as that of V_{21}; the latitudes of V_{32} (V_{32}'), V_{33} (V_{33}'), V_{34} (V_{34}'), V_{35} (V_{35}'), and V_{36} (V_{36}') are treated the same as the positive of the moon's declination if the angle between V_{31} and the moon is less than 90^o and the same as the negative of the moon's declination if the angle is greater than 90^o, their longitudes are designed to have a difference of 15^o, 0^o, -15^o, -30^o, and -45^o towards the longitude of V_{31}; the latitudes of V_{43} (V_{43}'), V_{44} (V_{44}'), V_{45} (V_{45}'), and V_{46} (V_{46}') are treated the same as the positive of the moon's declination if the angle between V_{42} and the moon is less than 90^o and the same as the negative of the moon's declination if the angle is greater than 90^o, their longitudes are designed to have a difference of 10^o, 5^o, 0^o, and -5^o towards the longitude of V_{42}. Once the geographic latitudes and longitudes of these sites are determined, the distance between any of these sites and the earth's centre may be calculated through Eq. (1), (2), and (3). And then, O_1V_{13} - O_1V_{12} + O_1V_{12} - O_1V_{11}, O_1V_{22} (O_1V_{22}') - O_1V_{21}, O_1V_{32} (O_1V_{32}') + O_1V_{33} (O_1V_{33}') + O_1V_{34} (O_1V_{34}') + O_1V_{35} (O_1V_{35}') + O_1V_{35} (O_1V_{35}') - $O_1V_{31,}$ and O_1V_{43} (O_1V_{43}') + O_1V_{44} (O_1V_{44}') + O_1V_{45} (O_1V_{45}') + O_1V_{46} (O_1V_{46}') - O_1V_{42} + O_1V_{42} - O_1V_{41} approximately represent the variations of water level at site V_{11}, V_{21}, V_{31}, and V_{41}. We see, V_{12} and V_{42} just play the role of connecting points. In the experiment of the oscillating vessel we found that with the passage of time, the rise or fall of water level at one end are no longer simultaneous with the fall or rise of the end. There is often a time lag between them. This lag is well consistent with the age of tide. The time lag is also considered for all these vessels. The reason for this delay is likely to be due to the inertia of transferring water that is globally enacted. The deformation of solid earth we propose, would require gravity to vary from site to site. Three sites (Strasbourg, Sutherland, and Apache Point) are selected to examine this expectation. Gravity variation (g) is calculated by a formula $g \sim 1/r^2\text{-}1/a^2$, r is the distance between any of three sites and the earth's centre, which can be got through formulas (1), (2), and (3) if the geographic latitudes and longitudes of these sites are known, a is the mean radius of the earth. The simulated and observed tides (gravity variation) are shown in Fig. 6 (b and c). Related parameters used in the simulation are listed in Table 1. On the whole, the simulated results are morphologically consistent with the observed results. But for a more exactly tide prediction, some factors such as the shape of ocean basin, orientation of coastline, water depth, Coriolis effect, inertia, and so on should be considered. In particular, when ocean basin is divided into some smaller vessels, the input of water from adjacent vessels needs to be included, this is because the travelling water may be refracted/reflected to enter from one vessel to another.

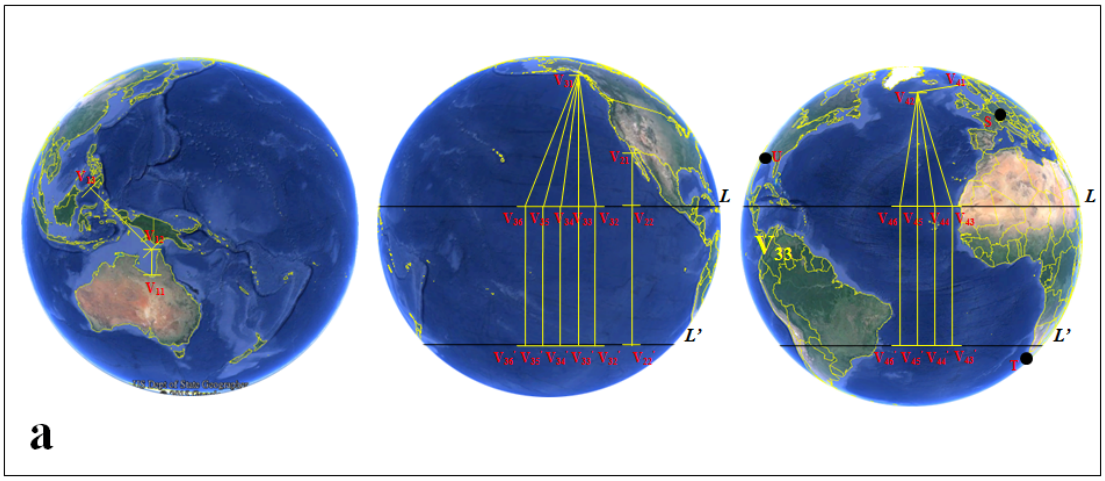
L
L'
L
L'
a

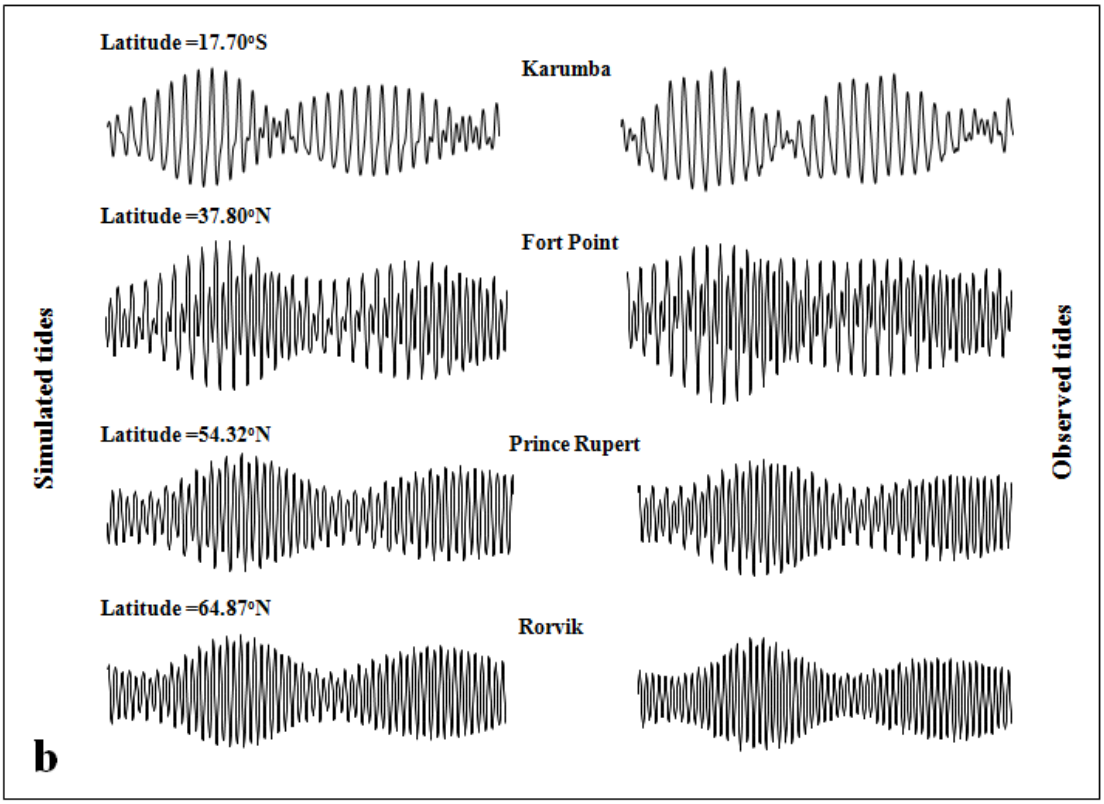
Latitude =17.70°S
Karumba
Latitude =37.80°N
Fort Point
Latitude =54.32°N
Prince Rupert
Latitude =64.87°N
Rorvik
Simulated tides
Observed tides
b

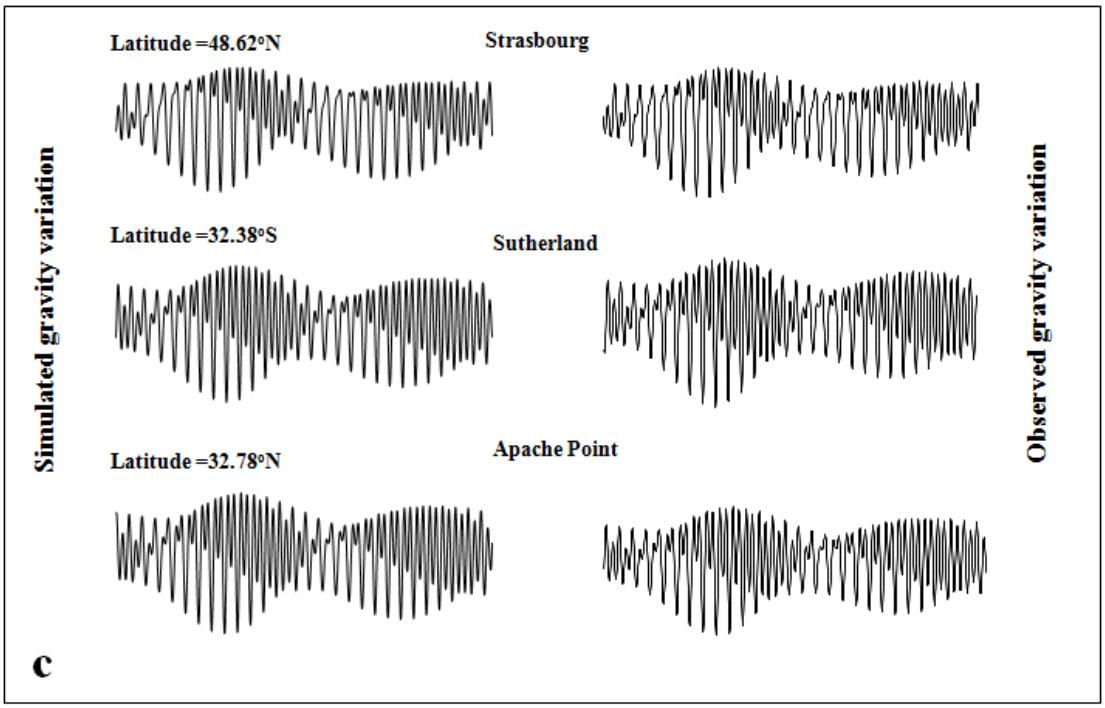

FIG. 6. Treatments of ocean vessels and comparisons of simulated and observed results. a, defining a smaller vessels within ocean basins and putting GGP (Global Geodynamics Project) sites at the surface of a solid earth (base map is from Google earth). V_{11}, V_{12}, …, represent the ends of the wanted vessels. Each rectangular box represents a smaller vessel. S, T, and U represent three gravity observational sites. *L* and *L*' are the expected paths that the earth-moon line tracks the earth, which give the latitudinal scope of the maximum rising point; **b**, showing a morphological comparison of the simulated and observed tides without scale in August 2014. In the simulation time lag for Fort Point is 2.0 hours, and for Prince Rupert, which involves fives partners, is an average 2.0 hours. The age of tide is commonly accepted as about 2 days; **c**, showing a morphological comparison of the simulated and observed gravity variations. Time span for all these simulations is from UTC 2014-08-01 00:00:00 to 2014-08-30 23:00:00. Data supporting is from NASA's JPL, GLOSS database - University of Hawaii Sea Level Center, Bureau National Operations Centre (BNOC) of Australia, and GGP (Global Geodynamics Project).

Table 1 Parameters selected for simulation

The Moon			Symbol
	Mass	$7.35*10^{22}$ kg (Wieczorek et al, 2006)	M_m
	Perigee	362600 km	R_{mp}
	Apogee	405400 km	R_{ma}
The Earth			
	Mass	$5.97*10^{24}$ kg (Luzum et al., 2011)	M_e
	Mean radius	6370 km (Lide, 2000)	a
	Mean distance from Sun	$1.49*10^{8}$ km (Simon et al., 1994)	R_s
The Sun			
	Mass	$1.99*10^{30}$ kg (Williams, 2013)	M_s
Geographic sites for water vessels		Latitude, Longitude	
	Karumba, Austrilia	17.70°S, 139.20°E	V_{11}

Partner (1)	13.00°S, 141.00°E	V_{12}
Partner (2)	5.00°N, 121.00°E	V_{13}
Fort Point, San Francisco, USA	37.80°N, 122.47°W	V_{21}
Partner (1)	__, 122.47°W	$V_{22}(V_{22}')$
Prince Pupert, Canada	54.32°N, 130.32°W	V_{31}
Partner (1)	__, 115.32°W	$V_{32}(V_{32}')$
Partner (2)	__, 130.32°W	$V_{33}(V_{33}')$
Partner (3)	__, 145.32°W	$V_{34}(V_{34}')$
Partner (4)	__, 160.32°W	$V_{35}(V_{35}')$
Partner (5)	__, 175.32°W	$V_{36}(V_{36}')$
Rorvik, Norway	64.87°N, 11.25°E	V_{41}
Partner (1)	50.00°N, 28.00°W	$V_{42}(V_{42}')$
Partner (2)	__, 18.00°W	$V_{43}(V_{43}')$
Partner (3)	__, 23.00°W	$V_{44}(V_{44}')$
Partner (4)	__, 28.00°W	$V_{45}(V_{45}')$
Partner (5)	__, 33.00°W	$V_{46}(V_{46}')$
Geographic sites for gravity	Latitude, Longitude	
Strasbourg, France	48.62°N, 7.68°E	S
Sutherland, South Africa	32.38°S, 20.82°E	T
Apache Point, New Mexico, USA	32.78°N, 105.82°W	U

On the whole, the water in the ocean basin undergoes two sets of overwhelming transferring per day: one is between site W and these sites (represented by *a*, *b*, *c*, and *d*) in line *L*, another is between site W and these sites (represented by *e*, *f*, *g*, and *h*) in line *L*'. The inflow of water naturally leads to the increase of water level, whereas the outflow of water leads to the decrease of water level. This finally gives site W two high waters and two low waters during a day. When the oscillation of ocean basin is associated with the positions of the moon, sun, and earth that mechanically control the deformation of solid earth, the two sets of water transferring becomes maximum at the times of full and new moon and minimum at the times of first quarter and last quarter, this generates two cycles of high and low waters during a lunar month.

5. Discussion

The mechanism of the oscillating water vessel is also applicable to the matter of an enclosed sea/lake. If we treat the Black sea as a vessel and use Eq. (1), (2), and (3) to estimate, the west or east end of this sea may experience a tide of about 12.0 cm. Similarly, a tube of water (20 m in length) horizontally located at equator will experience a tide of about 2.2×10^{-3} mm, an imperceptible amount. This means that, any small vessel, such as swimming pool, water cup, water bowl, and so on, because of its short size, wouldn't undergo a perceptible tide. The oscillating ocean basin drives water to move, continental shorelines are long enough to block the transferring water to form large accumulations. In particular, most of the shorelines are concave, this also may

create an effect of a narrow to amplify tide. Typical representatives are the tides around Qiantang River and the Bay of Fundy. In contract, the shorelines of the islands that are fully isolated in the deep oceans are short, the transferring water can't be accumulated and may be bypassed. These cause larger tidal ranges to occur at the coastal seas and smaller ones at the deep oceans. The rotating deformed solid earth causes ocean water to move back and forth. The transferring water, if constrained by the narrowness of a strait, may form a swift current, like that in the Cook Strait (Stevens et al. 2012; Bowman et al. 1983). For the various features of the tides in the Atlantic and in the North West Europe shelf seas, they may be understood as follows: the rise and fall of each part of the ocean basin is oriented from east to west as the earth spins, the rising of the east end of the Atlantic basin first leads water to flow towards the north, west, and south, the following rise of the middle part of the Atlantic basin leads water to flow towards east, north, west, and south, and finally, the rise of the west end of the Atlantic basin leads water to flow towards the north, east, and south. The westerly water may reach the eastern coastline of America nearly at the same time and leaves no difference in tidal phase. The northerly water may form a progression of tidal phases oriented north in the North Atlantic. Furthermore, a large body of north-easterly water would enter the strait of Gibraltar and cross the Celtic Sea, from where it would continue to run into the English Channel and other related regions. A series of progressive tides along the shores of these regions are created, such as the tides around England's shores. In time, the Atlantic ocean basin begins to fall from east to west, and water is slowly restored. On the whole, the falling of the middle of the Atlantic basin would lead water to flow in. This may give rise to a progression of tidal phases towards the north in the South Atlantic and towards the south in the North Atlantic. However, tidal observations appear to show the progression of tidal phases towards the south are not as apparent as towards the north. This could be ascribed to the influences of the trumpet-shape North and South Atlantic. The width of the North Atlantic reaches 6400 km at 22^{o} N and 3500 km at 52^{o} N, similarly, the width of the South Atlantic reaches 3800 km at 5^{o} S and 5500 km at 33^{o} S. The southerly water at the North Atlantic and at the South Atlantic may be decompressed and minimize the phases as the channel becomes wide. In contrast, the northerly water at the South Atlantic and at the North Atlantic would be narrowed to amplify the phases as the channel becomes narrow.

Newton in his book *Mathematical Principles of Natural Philosophy* described a tide (Proposition XXIV. Theorem XIX, translated by Andrew Motte): "*An example of all which Dr. Halley has given us, from the observations of seamen in the port of Batsham, in the Kindom of Tunquin (presently Viet Nam), in the latitude of $25^{o}50'$ north. In that port, on the day which follows after the passage of the moon over the equator, the waters stagnate: when the moon declines to the north, they begin to flow and ebb, not twice, as in other ports, but once only every day: and the flood happens at the setting, and the greatest ebb at the rising of the moon. This tide increases with the declination of the moon till the 7^{th} or 8^{th} day; then for the 7 or 8 days following it decreases at the same rate as it had increased before, and ceases when the moon changes its declination, crossing over the equator to south. After which the flood is immediately changes into an ebb; and thenceforth the ebb happens at the setting and the flood at the rising of the*

*moon; till the moon, again passing the equator, changes its declination. There are two inlets to this port and the neighboring channels, one from the seas of China, between the continent and the islands of Leuconia; the other from the Indian sea, between the continent and the island of Borneo. But whether there be really two tides propagated through the said channels, one from the Indian sea in the space of 12 hours, and once from the sea of China in the space of 6 hours, which therefore happening at the 3d and 9^{th} lunar hours, by being compounded together, produce those motions; or whether there be any other circumstances in the state of those seas, I leave to be determined by observations on the neighbouring shores."*Newton gave an explanation for this tide but it was not verified. A similar tide also appears in the Australian Gulf of Carpentaria. The tide at this location reduce to zero when the moon's declination is zero, increasing to its largest values when the moon is at its greatest declination, either north or south of the equator. This kind of tide is presently called a diurnal tide. Here we demonstrate how this tide forms under the frame of the rotating deformed solid earth. As shown in Fig. 7, when the moon declines to the north, as the elongation of solid earth is always in the earth-moon line and tracks from east to west, the part of the northern hemisphere of solid earth is raised at the moon's rising, this leads water to flow out and the water level at the location (marked with Z) falls naturally. With the passage of time, the part of the southern hemisphere of solid earth is raised at the moon's setting. This leads water to flow out, at least there is a water transferring towards the north and the water level at Z rises. When the moon declines to the south, the part of the southern hemisphere of solid earth is raised at the moon's rising. This leads water to flow out, at least, there is a water transferring towards the north, the water level at Z rises. With the passage of time, the part of the northern hemisphere of solid earth is raised at the moon's setting. This leads water to flow out, and the water level at Z falls. This process eventually gives Z one high water and one low water per day. When the moon is about at the equator, the water transferring between the northern and southern hemispheres is slight, the water at Z become nearly motionless.

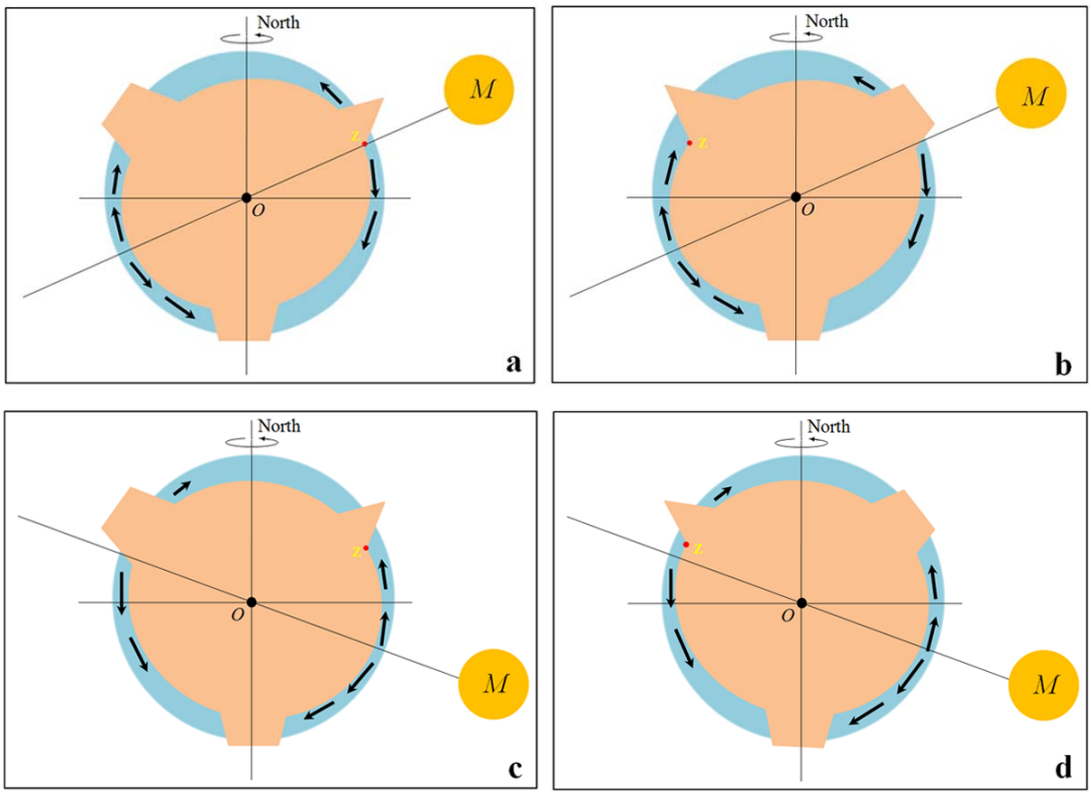

FIG. 7. Modelling the formation of diurnal tide in Batsham and Karumba (Z). From **a**(**b**) to **c**(**d**) the moon transfers from north to south. From **a**(**c**) to **b**(**d**), the earth rotates 180°. Please note, the deformation of solid earth is highly exaggerated. *M* represents the moon. Black arrows in each diagram denote water transfer caused by the elongation.

Galileo in his *Dialogue Concerning the Two Chief World Systems* (translated by Stillman Drake) described the tides of the Mediterranean, "*three varieties of these hourly changes are observed: in some places the waters rise and fall without making any forward motions; in others, without rising or falling they move now toward the east and again run back toward to the west; and in still others, the height and the course both vary. This occurs here in Venice, where the waters rise in entering and fall in departing. ... ..., elsewhere the water runs to and fro in its central parts without changing height, as happens notably in the Straits of Messina between Scylla and Charybdis, where the currents are very swift because of the narrowness of the channel. But in the open Mediterranean and around its islands, such as the Balearics, Corsica, Sardinia, Elba, Sicily (on the African side), Malta, Crete, etc., the alterations of height are very small but the currents are quite noticeable, especially where the sea is restrained between islands, or between these and the continent.*" The Mediterranean is like a perfect vessel of water. Under the effect of the deformation of solid earth, the vessel is shaken regularly, this yields water transferring between its related parts, refer to Fig. 4, the greatest alternation of water level occurs at the ends, whereas the smallest occurs in the open area. The travelling water, while constrained by the straits, form swift currents.

A critical difference between the attractive mechanism and this proposed theory lies at, the former relates ocean tide directly to the gravitational pulls of the moon and sun on the water, the latter relates ocean tide directly to the oscillation of ocean basin. Another difference is the former treats ocean tide and the deformation of solid earth (earth tide) separately, and the influence of earth tide on ocean tide is expressed with a function of diminishing factor ((1+k-h)Ωp/g, for instance), whereas the latter employs the deformation o solid earth to directly account for ocean tide. We see, this proposed theory not only may explain the general features of tide (two high waters and two low waters per day, the two cycles of high and low water per month, for instance), realize some competitive results with observations (tide and gravity), but also may avoid the problems of the equilibrium tide, most importantly, it provides a physical foundation for present tide prediction. We know, tide prediction is presently made from tide observation. As tidal variations (the height and time of high and low water) are recorded continuously at many locations, we use computers to analyze these records to identify some constituents of complex wave. This works out the wave heights and time lags of each of the many constituents. Once the timing, periodicity, and the amplitude of each constituent are obtained for a particular location, a simple addition of these constituents gives the tidal height at the future time (Segar 2012). However, this treatment of tidal prediction is mathematical but not physical. For a special site, the high water it undergoes represents an inflow of water from other places and the low water it undergoes represents an outflow of water towards other places as water is totally conservative, a simple addition of these constituents clearly hasn't tell where the water comes from and where the water goes. In contrast, this proposed theory reaches the point. As shown in Fig. 5, the water transferring between site W and any of those sites *b*, *c*, *d*, *f*, and *g* may be depicted with a wave, in which the direction of water movement is discernable, an addition of these waves realistically generates the variation of water level of site W. Anyway, these water transferrings would be reflected/refracted by landmass and deflected by the Coriolis force, essentially, they must follow the dynamic equations we already build in the established understanding.

Acknowledgements We thank Phil Woodworth, David Pugh, Walter Babin, Thierry De Mees, Roger A. Rydin, Duncan Agnew, and Wouter Schellart for comments on the original manuscript, we thank Hartmut Wziontek and Calvo Marta for discussions on gravity data, and we thank Mike Davis for providing tide data. We also thank these institutes (U.S. NOAA, NASA's JPL, GLOSS database - University of Hawaii Sea Level Center, Bureau National Operations Centre (BNOC) of Australia, and GGP (Global Geodynamics Project)) for their data supporting. These people (including Dr. John M. Huthnance, Dr. Neil Wells) whose researches relate to tidal theory could be potentially conflict of interest.

References

Agnew, D. C., 1981: Nonlinearity in rock - Evidence from earth tides. *J. geophys. Res.*, **86**, 3969-3978.

Birch, F., 1964: Density and Composition of Mantle and Core. *Journal of Geophysical Research Atmospheres*, **69(20)**, 4377-4388.

Bowman, M. J., A. C. Kibblewhite, R. A. Murtagh, S. M. Chiswell, B. G. Sanderson, 1983: Circulation and mixing in greater Cook Strait, New Zealand. *Oceanol. Acta.*, **6(4)**, 383-391.

Burša, M., 1993: Parameters of the earth's tri-axial level ellipsoid. *Studia Geophysica et Geodaetica*, **37(1)**, 1-13.

Cartwright. D. E., A. C. Edden, R. Spencer, J. M. Vassie, 1980: The tides of the northeast Atlantic Ocean. *Philosophical Transactions of the Royal Society of London*, **A298**, 87-139.

Cartwright, D. E., 1999: *Tides: A Scientific History*. Cambridge University Press.

Deacon, M., 1971: *Scientists and the Sea, 1650-1900*. Academic Press (London).

Doodson, A. T. and H. D. Warburg, 1941: *Admiralty Manual of Tides*. London HMSO.

Farrell, W. E., 1973: earth tides, ocean tides and tidal loading. *Philosophical Transactions of the Royal Society of London*, **A274**,253-259.

Fowler, C. M. R., 2004: *The Solid earth: An Introduction to Global Geophysics (2nd Education)*. Cambridge University Press.

Fu, L.-L. and A. Cazenave, 2001: *Satellite Altimetry and earth Sciences*. Academic Press, San Diego, Calif.

Gao, Z. Z., Y. B. He, X. D. Li, T. Z. Duan, 2013: Review of research in internal-wave and internal-tide deposits of China. *Journal of Palaeogeography*, **2 (1)**, 56-65.

Gargett, A. E., B. A. Hughes, 1972: On the interaction of surface and internal waves. *Journal of Fluid Mechanics*, **52**, 179-191.

Garrett, C., W. Munk, 1979: Internal waves in the ocean. *Annual Review of Fluid Mechanics*, **1**, 339-369.

Heiskanen, W. A., 1962: Is the earth a triaxial ellipsoid?. *J. geophys. Res.*, **67 (1)**, 321-327.

Hendershott, M. C., 1972: The effects of solid earth deformation on global ocean tides. *Geophysical Journal of the Royal astronomical Society*, **29**, 389-402.

Herndon, J. M., 1980: The chemical composition of the interior shells of the earth. *Proc. R. Soc. Lond.*, **A372(1748)**, 149-154.

Herndon, J. M., 2005: Scientific basis of knowledge on earth's composition. *Current Science*, **88(7)**, 1034-1037.

Jordan, T. H., 1979: Structural Geology of the earth's Interior. *Proc. Natl. Acad. Sci. USA.*, **76 (9)**, 4192-4200.

Kaula, W. M., 1968: *Introduction to Planetary Physics: the Terrestrial Planets*. John Wiley.

Kopal, Z., 1969: *Dynamics of the earth-moon System*. Springer Netherlands.

Lambeck, K., 1988: *Geophysical Geodesy*. Clarendon Press, Oxford.

Lide, D. R., 2000: *Handbook of Chemistry and Physics (81st ed.)*.

Longman, I. M., 1963: A Green's function for determining the deformation of the earth under surface mass loads. *J. geophys. Res.*, **68**, 485-496.

Love, A. E. H., 1909: The Yielding of the earth to Disturbing Forces. *Proc. Roy. Soc. London*, **82**, 73-88.

Luzum, B., and Coauthors, 2011: The IAU 2009 system of astronomical constants: The report of the IAU working group on numerical standards for Fundamental Astronomy. *Celestial Mechanics and Dynamical Astronomy*, **110(4)**, 293-304.

Melchior, Paul., 1974: earth Tides. *Surveys in Geophysics*, **1**, 275-303.

Monnereau, M., M. Calvet, L. Margerin, A. Souriau, 2010: Lopsided Growth of earth's Inner Core. *Science*, **328(5981)**, 1014-1017.

Munk, W., 1997: Once again-Tidal friction. *Progr. Oceanogr.*, **40**, 7-35.

National Research Council (U.S.)., 1964: *Panel on Solid earth Problems. Solid-earth Geophysics: Survey and Outlook*. National Academies.

National Research Council (U.S.)., 1993: *Solid-earth sciences and society*. National Academy Press, Washington.

Ozawa, H., F. Takahashi, K. Hirose, Y. Ohishi, N. Hirao, 2011: Phase Transition of FeO and Stratification in earth's Outer Core. *Science*, 3**34(6057)**, 792-794.

Pekeris, C. L. and Y. Accad, 1969: Solution of Laplace's equations for the M2 tide in the world oceans. *Philos. Trans. R. Soc. A.*, **A265**, 413-436.

Phillips, O. M., 1974: Nonlinear dispersive waves. *Annual Review of Fluid Mechanics*, **6**, 93-110.

Pidwirny, M., 2006: *Introduction to the Oceans (Fundamentals of Physical Geography, 2nd Edition)*.

Pugh, D. T., 1987: *Tides, Surges and Mean Sea-Level*. JOHN WILEY & SONS.

Pugh, D. T. and P. L. Woodworth, 2014: *Sea-Level Science: Understanding Tides, Surges Tsunamis and Mean Sea-Level Changes*. Cambridge Univ. Press, Cambridge.

Robert, H. S., 2008: *Introduction To Physical Oceanography*. Texas A& M University.

Roy, A. E., 1978: *Orbital Motion*. Adam Hilger, Bristol.

Schwiderski, E. W.,1979: Global ocean tides: Part II. The semidiurnal principal lunar tide 84 (M_2), Atlas of Tidal Charts and Maps. *NSWC Tech. Rep.*, 79-414.

Stammer, D., and Coauthors, 2014: Accuracy assessment of global barotropic ocean tide models. *Rev. Geophys.*, **52**, 243-282.

Stixrude, L. and R. E. Cohen, 1995: High-Pressure Elasticity of Iron and Anisotropy of earth's Inner Core. *Science*, **267 (5206)**, 1972-1975.

Scherneck, H.-G., 1991: A parametrized solid earth tide model and ocean tide loading effects for global geodetic baseline measurements. *Geophys. J. Int.*, **106(3)**, 677-694.

Schettino, A., 2014: *Quantitative Plate Tectonics*. Springer International Publishing.

Schureman, P., 1976: *Manual of Harmonic Analysis and Prediction of Tides*. United States Government Printing Office, Washington.

Segar, D. A., 2012: *Waves Introduction to Ocean Sciences (electric book), 2nd edition*.

Shanmugam, G., 2014: Review of research in internal-wave and internal-tide deposits of China: Discussion. *Journal of Palaeogeography*, **3**, 332-350.

Shepard, F. P., 1975: Progress of internal waves along submarine canyons. *Marine Geology*, **19**, 131-138.

Smart, W. M., 1940: *Spherical Astronomy*. Cambridge University Press.

Simon, J. L., P. Bretagnon, J. Chapront, M. Chapront-Touze, G. Francou, J. Laskar, 1994: Numerical expressions for precession formulae and mean elements for the moon and planets. *Astronomy and Astrophysics*, **282 (2)**, 663-683.

Stevens, C. L., M. J. Smith, B. Grant, C. L. Stewart, T. Divett, 2012: Tidal Stream Energy Extraction in a Large Deep Strait: the Karori Rip, Cook Strait. *Continental Shelf Research*, **33**, 100-109.

Vlasenko, V., N. Stashchuk, K. Hutter, 2005: *Baroclinic Tides: Theoretical Modeling and Observational Evidence*. Cambridge Univ. Press, Cambridge.

Visser, P. N. A. M., N. Sneeuw, T. Reubelt, M. Losch, T. Van Dam, 2010: Space-borne gravimetric satellite constellation and ocean tides: Aliasing effects. *Geophys. J. Int.*, 181, 789-805.

Wootton, A., 2006: earth's Inner Fort Knox. *Discover*, **27 (9)**, 18.

Wieczorek, M. A., and Coauthors, 2006: The constitution and structure of the lunar interior. *Reviews in Mineralogy and Geochemistry*, **60(1)**, 221-364.

Williams, D. R., 2013: *Sun Fact Sheet, NASA Goddard Space Flight Center*.